

Observation of sub-Doppler temperatures in bosonic magnesium

T. E. Mehlstäubler, K. Moldenhauer, M. Riedmann, N. Rehbein, J. Friebel, E. M. Rasel, and W. Ertmer
Institute of Quantum Optics, Leibniz Universität Hannover, Welfengarten 1, 30167 Hannover, Germany
(Received 25 November 2006; revised manuscript received 2 November 2007; published 12 February 2008)

Temperatures below the Doppler limit of 1.9 mK have been observed in magnesium. The strong cooling transition was modified by a coherent two-color excitation exploiting the longer lifetime of an upper level. We developed a theoretical model to describe the light forces and cooling originating from the induced quantum interference in a three-level system. Time-of-flight measurements verified temperatures of 500 μ K in a one-dimensional (1D) molasses in accordance with our theoretical model. By implementing this scheme in a 3D magneto-optical trap with a single ir beam, temperatures as low as 1 mK could be realized. For ideal conditions we extrapolate to temperatures of 50 μ K. With cooling times of about 1 ms, a fast and efficient cooling scheme was realized, particularly attractive for optical frequency standards.

DOI: 10.1103/PhysRevA.77.021402

PACS number(s): 37.10.De, 32.80.Wr, 37.10.Vz

Fostered by the invention of optical frequency combs [1,2], optical clocks based on neutral atoms or ions [3] are today developing into a new range of fractional instability and reproducibility beyond state-of-the-art cesium clocks [4]. Decisive ingredients for this progress are novel solutions tailored to atoms with narrow to ultranarrow optical transitions. Recent examples are the idea of the lattice clock [5–8], the quantum logic clock [9], and new cooling schemes (e.g., [10–13]). Among the candidates for optical clocks based on neutral atoms, Mg displays very attractive features, such as a low blackbody radiation shift [14], fermionic and bosonic isotopes of suitable abundance, long-lived states [15], and the existence of a magic wavelength, a prerequisite for the lattice clock. However, temperatures below the Doppler limit of 1.9 mK have never been reported for Mg—a limit that needs to be surpassed in order to reach higher stabilities for free falling atoms [16] as well as for the implementation of a lattice clock with Mg atoms. Quench cooling, an established technique to cool calcium atoms to the recoil limit [17,18], suffers from a low capture efficiency at available laser power and the increased initial atomic temperatures in a Mg magneto-optical trap (MOT) [19].

In this paper, we report on the observation of temperatures below the Doppler limit of 1.9 mK for the strong cooling transition $^1S_0 \rightarrow ^1P_1$ of ^{24}Mg . Our work was stimulated by the proposal from Magno *et al.* [12] to Doppler-cool alkaline-earth-metal atoms in a two-color molasses, exploiting the smaller linewidth and thus higher velocity selectivity of the excited state. We observed light forces that can be explained only by a theory additionally taking into account the coherences in the three-level system. An indication of this coherent cooling mechanism is the occurrence of temperature minima for both red and blue detuning from the two-photon resonance. A first experimental evidence for two-photon cooling was observed in the work by Malossi *et al.* [20], where a temperature reduction by a factor of 2.5 was indicated with a decreased MOT radius. For the laser intensities and detuning given in [20], the theoretically expected Doppler temperature of the Mg MOT was $T_D = 3$ mK. However, for the chosen MOT parameters, additional heating, especially observed in alkaline-earth-metal atoms, leads to temperatures in the Mg MOT that are 4–5 times higher than

this theoretical value [21]. Thus the great challenge remains of preparing large atomic samples at ultracold temperatures.

In our experiment, we have conducted time-of-flight (TOF) measurements to study the atomic temperatures and light forces, and compared them with our theoretical model. In a one-dimensional (1D) molasses configuration [22] temperatures as cold as 500 μ K, more than a factor of 10 lower than the initial temperature in the molasses, have been achieved, which are in excellent agreement with our theoretical work. With well-resolved magnetic substates in the 1D molasses we could observe quantum interference in the diamond scheme as predicted in [23]. We have also shown that this cooling scheme can be implemented in a MOT in the presence of strong magnetic fields. We demonstrated that temperatures of $T=1$ mK, well below the Doppler limit, can be achieved, by utilizing a regime of low uv saturation.

In Mg the fast-decaying 1P_1 state, for which standard Doppler theory predicts a temperature limit of 1.9 mK, can be coupled to the longer-lived 1D_2 state with an ir laser at 881 nm (Fig. 1). This scheme represents an almost closed three-level system with weak decay rates to the states 3P_2 and 3P_1 [15]. By coherently driving the two-photon transition, the narrow upper level is excited and the population in the intermediate level is modified [Fig. 2(a)], as in electromagnetically induced transparency [10]. This leads to a steeper force gradient of the uv molasses experienced by atoms with slow velocities [Fig. 2(b)]. In Mg, for our experimental parameters, the cooling force is dominated by the large recoil and high scattering rate of the uv photons. This

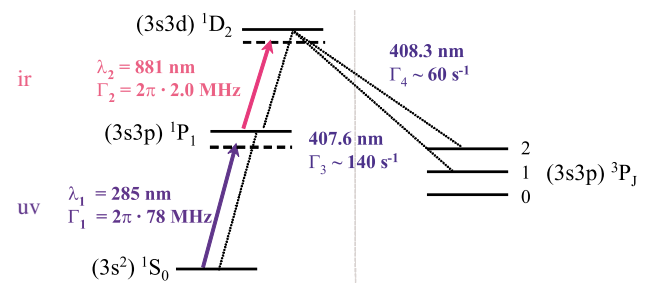
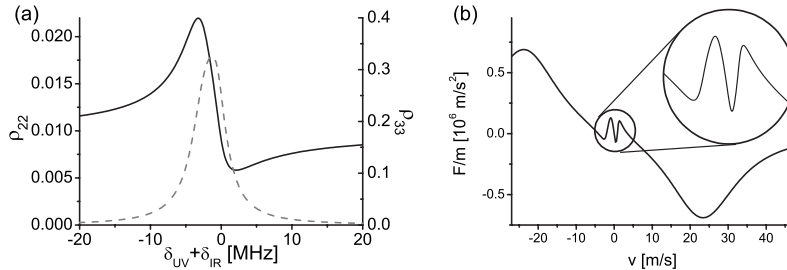


FIG. 1. (Color online) Simplified energy level diagram for ^{24}Mg . Radiative decay channels are shown with dotted lines.



allows a simple implementation of this cooling scheme, especially in three dimensions. A single ir laser beam is sufficient to modify the excitation probability of the intermediate state and thus provides enhanced cooling from all directions in the uv molasses. For a one-dimensional uv molasses with only one additional ir laser beam, we calculate the light force [24] as

$$F = \hbar k_1 \Gamma_1 (\rho_{22}^{(l)} - \rho_{22}^{(r)}) + \hbar k_2 \Gamma_2 (\rho_{33}^{(l)} - \rho_{33}^{(r)}). \quad (1)$$

Here, ρ_{22} and ρ_{33} represent the populations of the intermediate and upper states and the indices (l) (left) and (r) (right) denote the directions of the uv laser beams. They are dependent on the relative detunings $\delta_{21}^{(l)} = \delta_{uv} - v/\lambda_1$, $\delta_{21}^{(r)} = \delta_{uv} + v/\lambda_1$, and $\delta_{32} = \delta_{ir} - v/\lambda_2$, which include the Doppler shift and laser detuning with respect to the one-photon transitions. To derive the populations in the three-level system we follow the same mathematical approach previously used to model quench cooling [11] and extract the force profile in dependence on the atomic velocity [Fig. 2(b)]. The resulting temperature $T = D/k_B\alpha$ is determined by the friction coefficient $\alpha = -dF/dv|_{v=0}$ and the diffusion constant [22,24]

$$D = (\hbar k_1)^2 \Gamma_1 (\rho_{22}^{(l)} - \rho_{22}^{(r)}) + (\hbar k_2)^2 \Gamma_2 (\rho_{33}^{(l)} - \rho_{33}^{(r)}). \quad (2)$$

According to this model, the temperature limit is given by the linewidth of the upper level as about 50 μ K.

Our current MOT setup [25–27] delivers up to 10^8 cold Mg atoms at 4–5 mK. The ir light is provided by an external-cavity-stabilized Ti:sapphire laser with a linewidth below 1 MHz. Long-term stability is obtained by referencing the laser via a transfer cavity to a polarization-stabilized HeNe laser. The frequency of the two-photon transition is determined first by the decrease of the MOT fluorescence as atoms are excited to 1D_2 and subsequently decay into the metastable 3P_j states. Atoms in 3P_2 with a lifetime of 2200 s, are lost; atoms in 3P_1 decay after 5 ms and a fraction, dependent on the diameter of the MOT laser beams, can be recaptured. For typical parameters of the uv MOT a decrease in uv fluorescence of more than a factor of 20 was observed. The fluorescence of the ${}^1D_2 \rightarrow {}^3P_{2,1}$ transition at 408 nm was directly measured as well.

For our studies of two-photon cooling in one dimension, we prepared an atomic sample in a MOT and then switched off the lasers and the magnetic quadrupole field. After 200 μ s, two counterpropagating uv laser beams in combination with a single collinear ir laser beam were pulsed onto the free-falling atoms for 200 μ s. Typical saturations $s = I/I_{sat}$ per laser beam were $s_{uv} = 0.007$ and $s_{ir} = 980$. The frequency of the ir laser was varied around the two-photon resonance while δ_{uv} was kept fixed. A weak magnetic field of about 5 G nearly parallel to the molasses direction was present. After this cooling pulse the cloud freely expands for $t \approx 2$ ms and is imaged onto a charge-coupled device camera (TOF). A series of images at different expansion times (see, e.g., inset of Fig. 5), yields an accurate measure of the temperature with a relative uncertainty of 25%. The temperature of the pure 1D uv molasses without the ir laser is $T_{mol} = 5\text{--}6$ mK, slightly higher than the temperature in the MOT. This is attributed to imperfections in the uv molasses beam profile [28].

FIG. 2. (a) Populations ρ_{22} in the intermediate (solid line) and ρ_{33} in the upper level (dashed line) when δ_{ir} is varied and $\delta_{uv} = -80$ MHz. (b) Force exerted on the atoms for two counterpropagating uv beams and a single ir beam at $\delta_{ir} = 75$ MHz and $\delta_{uv} = -80$ MHz.

We investigated quantum interference in the diamond scheme as predicted in [23] and demonstrated the ability to coherently drive the two-photon transition in the presence of magnetic fields. For this we scanned the ir laser frequency ν_{ir} across the two-photon resonances and varied the laser polarizations [see Figs. 3(a) and 3(b)]. The frequencies of the two-photon resonances can be determined from the size and shape of the cloud after the TOF. Already here cooling for both blue- and red-detuned ir laser light is indicated. The linear polarization of the uv laser is perpendicular to the magnetic field. Thus, it is decomposed into σ^+ and σ^- , which enhances transitions with $\Delta m = \pm 1$ and suppresses transitions with $\Delta m = 0$. The resulting nine-level scheme is shown in Fig. 3(c). For Fig. 3(a) the polarizations of uv and ir are parallel, so the two paths to the $m=0$ state interfere constructively, and clearly all three resonances corresponding to the different excitation paths can be resolved. For Fig. 3(b) the polarization of the ir laser was rotated by 90°. This shifts the

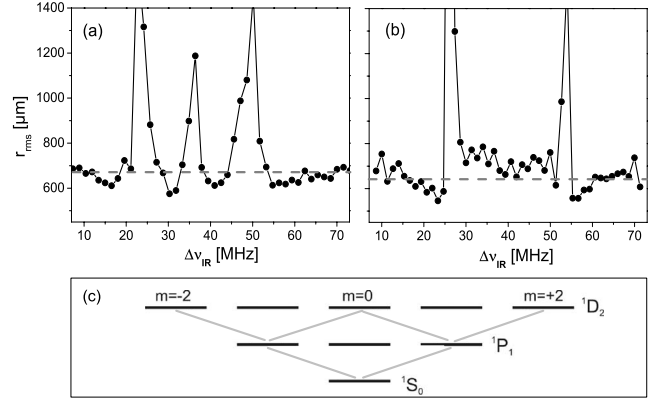


FIG. 3. Radii of the atom cloud after free expansion $\Delta_{uv} = -40$ MHz. The radius without ir laser is depicted by the dashed line. In (a) polarizations of uv and ir are parallel; in (b) they are orthogonal. Hence the excitation paths in the diamond scheme to 1D_2 , $m=0$, shown in (c), destructively interfere.

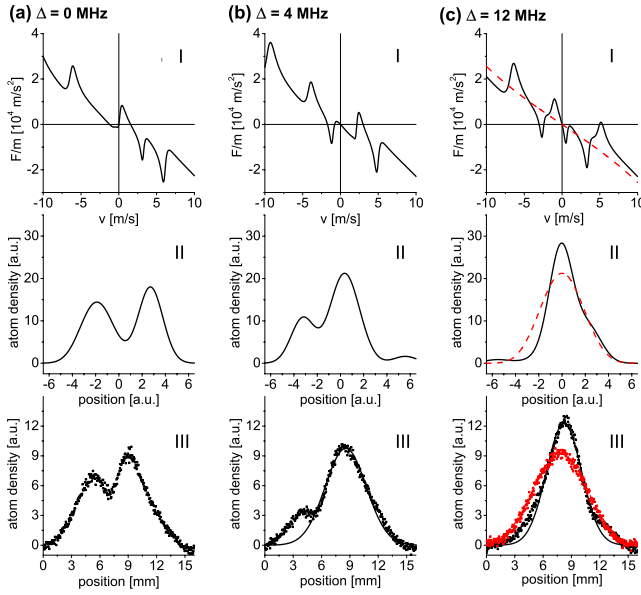


FIG. 4. (Color online) Force profile (I) and calculated (II) and measured (III) atom distribution for three different detunings Δ . In (c) values for a uv molasses are shown in red (dashed) for comparison. Solid lines in III are Gaussian fits.

phase of the two excitation paths to the ${}^1D_2, m=0$ state by π with respect to each other and they interfere destructively. Excitation to ${}^1D_2, m=0$ is suppressed as predicted for the diamond scheme [23]. In the following experiments the polarizations are chosen to be parallel.

Our time-of-flight technique allows us to study the effect of the uv light forces, modified by the ir beam, on the atoms. For comparison with our theory, we calculate the expected atom distributions after the interaction with the two-photon molasses light. Three resonances were included in an extended version of our model to account for the different magnetic sublevels. Due to imperfections of the beam adjustment and small angles between the magnetic field and the polarization of the laser light, the Rabi frequency of the ir transition is assumed to be reduced by 20%. The Zeeman effect leads to a splitting of 15 MHz between the observed resonances. Figure 4 shows a comparison between the experimental data and our model. The columns correspond to three different detunings relative to the two-photon resonances, $\Delta = \delta_{uv} + \delta_{ir}$. Here, $\delta_{uv} = -80$ MHz was kept fixed and Δ defined to be 0 for the $m=0 \rightarrow m=-2$ resonance. For each detuning the calculated modified forces (I), modeled atomic cloud profiles (II), and experimentally observed atomic distribution after 1.9 ms of free expansion (III) are shown. In our model, the force I acts on a Gaussian atomic cloud and the atoms expand freely according to their new velocities. In Fig. 4(a) the lasers are resonant with the two-photon transition $m=0 \rightarrow m=-2$. Due to the positive slope of the force profile at $v=0$, atoms at rest are accelerated, which corresponds to the central dip in the atomic distribution [see Fig. 4(a)]. The force profile leads to bunching of these atoms around $v \approx \pm 1$ m/s which is confirmed by the TOF. Figures 4(b) and 4(c) show two-photon cooling for different detunings close to resonance. Depending on the initial atomic tem-

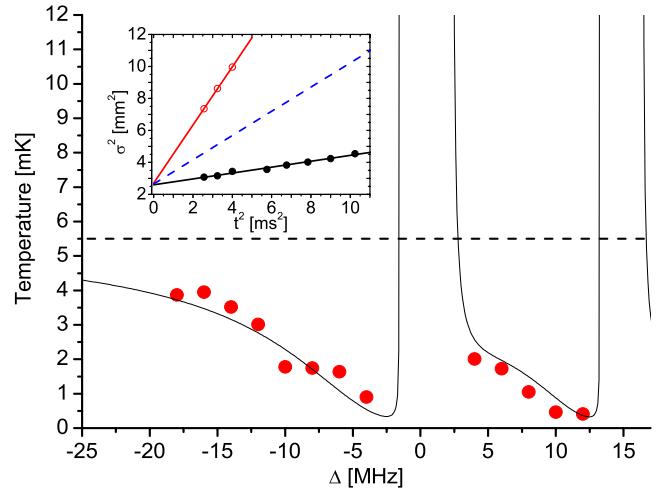


FIG. 5. (Color online) Temperature obtained by TOF spectroscopy (dots) and simulation (solid line) after 1D two-photon molasses cooling. For large Δ , temperatures approach T_{mol} , the temperature of the pure uv molasses (horizontal line). The inset shows the TOF data at T_{mol} (red, open circles) and a two-photon molasses at $T = 500 \mu\text{K}$ (black). The blue, dashed line represents $T_D = 2.2 \text{ mK}$.

perature and specific ir detuning, cooling is enhanced for a part of the atoms due to a larger α . Faster atoms at velocities where the light force reverses sign are accelerated and cooled into a moving frame. For optimum detuning 85% of the atoms can be cooled to $T = 500 \mu\text{K}$ around velocity zero [Fig. 4(c)]. The rest of the atoms remain in the side wings of the new atomic velocity distribution. The good agreement between calculated and measured atomic cloud profiles allowed us to calibrate δ_{ir} and locate the exact frequency of the two-photon resonances.

We compared the predictions of our model in 1D with the temperatures deduced from our TOF measurements (Fig. 5). The detunings Δ in Figs. 4 and 5 are directly comparable. The theoretical temperatures have been scaled with a factor T_{mol}/T_D to account for the observed additional heating in the pure uv molasses, assuming a constant additional heating rate. Here $T_D = 2.2 \text{ mK}$ is the Doppler temperature for $\delta_{uv} = -80 \text{ MHz}$ and $s_{uv} = 0.007$ [22]. In accordance with the model, the lowest temperature could be observed at a red detuning of a few megahertz to the central resonance. The corresponding TOF spectrum is shown as an inset. The measured temperatures as low as $500 \mu\text{K}$ are a factor of 4.5 below the Doppler temperature and a factor of 10 smaller than the temperatures we can obtain in our 1D uv molasses.

Coherent two-photon cooling was also implemented in a 3D uv MOT. Initial temperatures in the MOT, operated at $\delta_{uv} = -\Gamma_1/2\pi$ and extremely weak uv power $s_{uv} = 0.007$ per beam, were about 3.8 mK, while the expected theoretical Doppler temperature for this detuning is 2.4 mK. We compared running-wave and standing-wave configurations for the ir laser with $s_{ir} \approx 700-1000$ per beam. Near the two-photon resonance the fluorescence is drastically reduced due to the decay into dark metastable states [Fig. 6(c)], if the atoms are exposed for longer than 1 s to the ir light. Due to the strong light forces of two-photon cooling, however, an ir

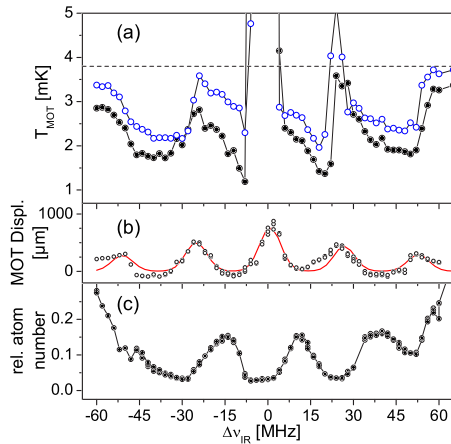


FIG. 6. (Color online) (a) T_{MOT} after 57 ms of two-photon cooling with one (open blue circles) and two (full circles) ir beams present. The dashed line marks the initial MOT temperature. At long interaction times ($\gg 1$ s) displacement of the MOT (b) and atom loss (c) are observed. Atom numbers are relative to the atom number without ir laser.

pulse of 1 ms duration is sufficient to reach steady-state temperature, and no atoms are lost during the cooling process.

In the magnetic quadrupole field of the MOT, all five Zeeman sublevels of 1D_2 are excited, resulting in five two-photon resonances. For the running-wave configuration the position of the trapped atom cloud is very sensitive to the two-photon detuning and was used to determine the position of the two-photon resonances [solid line, Fig. 6(b)]. This yielded a Zeeman splitting of 26 MHz and corresponds to a MOT displaced at an offset field of 19 G due to the imbalance of our retroreflected MOT beams. Close to the resonances, the temperature T_{MOT} increases [Fig. 6(a)] and, for long ir exposure, the number of atoms in the MOT is drasti-

cally reduced [Fig. 6(c)]. Cooling was observed on both sides of each resonance, while T_{MOT} for retroreflected ir beams was generally lower due to the higher ir saturation. The lowest temperature of 1.0 mK, well below the Doppler limit of Mg, was achieved by slightly red detuning from the central resonance, and more than 60% of the atoms could be transferred.

In conclusion, we have demonstrated temperatures of Mg atoms below the Doppler limit of 1.9 mK. Applying two-photon cooling in a 1D molasses, temperatures as low as 500 μK were achieved, ten times lower than the initial atom temperature. For a 3D MOT, despite the presence of strong magnetic field gradients, $T_{\text{MOT}}=1.0$ mK could be observed. Temperatures in the molasses and uv MOT were limited by the beam profile of the uv beams, which led to a constant higher diffusion rate. Without this technical heating we extrapolate to temperatures of 200 and 600 μK in the 1D molasses and MOT configuration, respectively. Our model, as well as related work [29,30], indicates that the lifetime of the upper state limits the achievable temperature to about 50 μK . The demonstrated cooling scheme allows for rapid cooling of ground state singlet atoms to millikelvin temperatures with cooling times of $t \approx 1$ ms. Loss into dark states is avoided by the short cooling time. In order to cool 100% of the atoms to zero velocity, a frequency chirp of the ir laser can be applied. This, on one hand, opens the way toward a Mg-based optical frequency standard with a short-term fractional frequency instability of 10^{-15} in 1 s [16]. On the other hand, it delivers a rapid precooling scheme for optical clock candidates that need to efficiently prepare ultracold atoms by quench cooling or for a rapid loading into a dipole trap.

This work has been supported by the DFG under SFB407 and EGC. We thank Veronica Ahufinger and Giovanna Morigi for helpful discussions.

-
- [1] T. Udem, J. Reichert, R. Holzwarth, and T. W. Hänsch, Phys. Rev. Lett. **82**, 3568 (1999).
 [2] S. A. Diddams *et al.*, Phys. Rev. Lett. **84**, 5102 (2000).
 [3] P. Gill, Metrologia **42**, 125 (2005).
 [4] R. Wynands and S. Weyers, Metrologia **42**, S64 (2005).
 [5] M. Takamoto *et al.*, Nature (London) **435**, 321 (2005).
 [6] A. D. Ludlow *et al.*, Phys. Rev. Lett. **96**, 033003 (2006).
 [7] Z. W. Barber *et al.*, Phys. Rev. Lett. **96**, 083002 (2006).
 [8] R. Le Targat *et al.*, Phys. Rev. Lett. **97**, 130801 (2006).
 [9] P. O. Schmidt *et al.*, Science **309**, 749 (2005).
 [10] G. Morigi, J. Eschner, and C. H. Keitel, Phys. Rev. Lett. **85**, 4458 (2000).
 [11] T. E. Mehlstäubler *et al.*, J. Opt. B: Quantum Semiclassical Opt. **5**, S183 (2003).
 [12] W. C. Magno, R. L. Cavasso Filho, and F. C. Cruz, Phys. Rev. A **67**, 043407 (2003).
 [13] T. H. Loftus, T. Ido, A. D. Ludlow, M. M. Boyd, and J. Ye, Phys. Rev. Lett. **93**, 073003 (2004).
 [14] S. G. Porsev and A. Derevianko, J. Exp. Theor. Phys. **102**, 195 (2006).
 [15] S. G. Porsev, M. G. Kozlov, Y. G. Rakhlina, and A. Derevianko, Phys. Rev. A **64**, 012508 (2001).
 [16] J. Keupp *et al.*, Eur. Phys. J. D **36**, 289 (2005).
 [17] E. A. Curtis, C. W. Oates, and L. Hollberg, Phys. Rev. A **64**, 031403(R) (2001).
 [18] T. Binnewies *et al.*, Phys. Rev. Lett. **87**, 123002 (2001).
 [19] N. Rehbein *et al.*, Phys. Rev. A **76**, 043406 (2007).
 [20] N. Malossi *et al.*, Phys. Rev. A **72**, 051403(R) (2005).
 [21] F. Y. Loo *et al.*, J. Opt. B: Quantum Semiclassical Opt. **6**, 81 (2004).
 [22] P. D. Lett *et al.*, J. Opt. Soc. Am. B **6**, 2084 (1989).
 [23] G. Morigi, S. Franke-Arnold, and G. L. Oppo, Phys. Rev. A **66**, 053409 (2002).
 [24] W. Rooijakers, W. Hogervorst, and W. Vassen, Phys. Rev. Lett. **74**, 3348 (1995).
 [25] T. E. Mehlstäubler, Ph.D. thesis, Universität Hannover, 2005.
 [26] K. Sengstock *et al.*, Appl. Phys. B: Lasers Opt. **59**, 99 (1994).
 [27] E. M. Rasel *et al.*, J. Opt. Soc. Am. B (to be published).
 [28] T. Chaneliere *et al.*, J. Opt. Soc. Am. B **22**, 1819 (2005).
 [29] G. Morigi and E. Arimondo, Phys. Rev. A **75**, 051404(R) (2007).
 [30] J. W. Dunn *et al.*, e-print arXiv:physics/0610272.